China Ocean Eng., Vol. 26, No. 1, pp. 123 – 138

DOI 10.1007/s13344-012-0009-1, ISSN 0890-5487

A Long-Term Numerical Model of Morphodynamic Evolution and Its Application to the Modaomen Estuary

MO Wen-yuan (莫文渊)[a, b, 1], WEI Xing (韦　惺)[c] and QIU Li-guo (邱立国)[a, b]

[a] *School of Environmental Science and Engineering of Sun Yat-Sen University, Guangzhou 510275, China*

[b] *Hainan Marine Development Plan and Design Institute, Haikou 570125, China*

[c] *Key Laboratory of Tropical Marine Environmental Dynamics, South China Sea Institute of Oceanology, Chinese Academy of Sciences, Guangzhou 510301, China*

(Received 16 February 2011; received revised form 22 August 2011; accepted 9 October 2011)

ABSTRACT

Because of the influence of human activities, the evolution of the Modaomen Estuary is no longer a purely natural process. We used a long-term morphodynamic model (PRD-LTMM-10) to study the evolution of the estuary from 1977 to 1988. The model incorporated modules for riprap-siltation promotion and waterway dredging. The model can simulate the morphodynamic evolutionary processes occurring in the Modaomen Estuary during the period of interest. We were able to isolate the long-term influences of various human engineering activities and the roles of natural factors in estuarine evolution. The governance projects had the largest effect on the natural development of the estuary, resulting in larger siltation on the west side. Installation of riprap and reclamation of submerged land resulted in scouring of the main Hengzhou Channel causing deep trough out-shift. Severe siltation narrowed the upper end of the Longshiku Deep Trough.

Key words: *Modaomen Estuary*; *long-term model*; *evolution*

1. Introduction

Because of their unique geographical location and abundance of natural resources, estuaries have long been the focus of human exploitation and utilization. As a result, the processes driving estuarine evolution are no longer purely natural. Given this, the influence of human activities on the geomorphological evolution of nearshore estuaries has attracted widespread attention amongst researchers. Up to date, the long-term geomorphological variation in nearshore estuaries has primarily been studied by use of comparative analyses based on historical charts, topographic survey data, satellite remote sensing data, and GIS. For example, van der Wal *et al*. (2002) used a combination of historical charts, topographic survey data, and remote sensing data to document topographic changes in the Ribble Estuary in the northwest England and determine the effect of human influence during the past 150 years. Similarly, Jaffe *et al*. (2007) used a series of historical water depth data to evaluate the topographic evolution of the San Pablo Bay, California from 1856 to 1983. Stanica *et al*. (2007) compared field measurements and historical charts to evaluate changes in topography and sediment transport in the Sulina Estuary,

1 Corresponding author. E-mail: redondomo@163.com

Danube as a result of human activities during the past 150 years. The evolutionary processes and trends in historical geomorphology in a given estuary are most easily explained by the aforementioned methods. However, the influence of human activities on the morphodynamic processes and mechanisms controlling topographic evolution cannot be measured quantificationally by these techniques. This is particularly true for the small-scale processes (e.g. fluid dynamics, sediment transport, and sedimentary erosion) that cause long-term variation.

For better prediction of future topographic variation, sediment deposition characteristics and the effects of human activities on the nearshore estuary, it is important to understand the dominant factors that cause changes in estuarine topography. In addition, a range of tools for assessment and prediction at different temporal and spatial scales are also required for the management of the nearshore estuary environment. At smaller temporal and spatial scales, satisfactory results can be achieved by hydrodynamics and other process-based models for prediction (Pritchard *et al*., 2002). However, generating predictions over a larger time scale (10~100 years) or over a wider area requires the use of different methods, such as the "top-down" model and the "hybrid" model (Pritchard *et al*., 2002; Whitehouse, 2001; Townend, 2005). Simon *et al*. (2006) used two "top-down" methods, "Historical Trend Analysis" (HTA) and "Expert Geomorphological Assessment" (EGA), to quantitatively analyze the topographic evolution and changes in sedimentary volume in the Mersey Estuary during the last 150 years. HTA focuses primarily on the analysis of historical data for identifying and predicting trends in future development. However, it does not reveal the factors resulting in the topographic evolution and variation in sedimentary volume in the estuary. Long-term numerical models that utilize process-based simulation not only have the predictive ability of general mathematical models, but also aid the understanding and identification of event occurrence processes. Based on the physical background analysis of simulated events, this model is coupled with the calculation of small-scale hydrodynamics, sediment transport, and sedimentary erosion, to simulate or predict morphodynamic changes over a longer time scale led by certain control or reduction approaches. The objectives of long-term research is focused primarily on shoreline changes, balance adjustment of the coastal profile (Dean, 1991), closure of tidal channels, empirical equilibrium relationships, and marine basin filling (Quiquerez *et al*., 2000; O'brien, 1969; Bruun and Gerritsen, 1960). In these analyses, the stimulated time scales range from mid-length (season-year) to very long (geochronology). The model PRD-LTMM (Wu *et al*., 2006a, 2006b, 2007a; Wei *et al*., 2008; de Vriend *et al*., 1993; Latteux, 1995) has been used to study the topographic evolution of the Pearl River Delta during the last 6 ka BP. The model is one of the more commonly used process models having a long time scales (larger than a millennium). Although the model is also based on the classical Reynolds Equation, a special control technology has been introduced in the long-term calculation framework of PRD-LTMM, which ensures the rationality of a hybrid model when dealing with sedimentation flux and spatial distribution. The method for verification of this model also differs from that of the general long-term models. The output from PRD-LTMM has made a seminal contribution to the simulation of millennial-scale topographic evolution, filling a gap in long-term process models in both temporal (millennium) and spatial (delta evolution) scales.

With the basic framework of PRD-LTMM, a derivative model, PRD-LTMM-10, was developed to

model topographic evolution of a 10~100 year scale. We used this model to simulate topographic evolution in the Modaomen Estuary, Pearl River to evaluate the influence of human activities from 1977 to 1988.

2. PRD-LTMM-10 Model

2.1 Model Simplification

The mathematical model for long time scales begins with the calculation of water flow and sediment movement at a short time scale. However, the data for long time scales cannot be obtained by continuous calculation of common mathematical model over a short time scale, primarily due to the following reasons: (1) such calculations cannot be easily processed using currently available technology and (2) the input conditions and the "interference factors" generated in the calculation may be amplified resulting in a decrease in accuracy. Thus, the success of long-term morphodynamic models depends largely on the reduction and integration of different time scales (Wu *et al*., 2007b). The simplification of complex information is therefore a key issue for long-term simulations (Ren and Wu, 2006). In these instances, there may be multiple levels of simplification, including input simplification, physical system or model simplification, and output simplification. The effect of each level of simplification may also be reflected in differing ways in the output.

2.1.1 *Input Simplification*

Input simplification refers not only to the filter for model boundary conditions, but also includes the approximation of a number of parameters (e.g. roughness and diffusion coefficient) with small variations in long-term processes. The simplification of boundary input data involves the omission of events or processes that have only a small effect on topographic variation over a long time scale. This results in significant savings in computation and calculation time.

Long-term topographic evolution is the product of flow and sediment dynamics in various boundary conditions. Tides and waves have characteristic time scales that vary from seconds to months. The subtle processes associated with tidal action may not be considered in numerical models over long time scales. Typically, methods are incorporated to replace the entire tidal cycle with that of a minimum tide (Saros cycle with a year or 18.6 years) so that the effect on bed topography most closely models that of the actual tidal cycle. De Vriend *et al*. (1993) and Latteux (1995) noted that the tidal range of the representative tide is slightly larger than the average (7%~20%). De Vriend *et al*. (1993) and Latteux (1995) also calculated the sediment transport rate of the representative tide and the average transport rate for the corresponding observed tide over a long time scale. If both are equal (or approximately equal) in size and direction, the simulated interval is assumed to represent the actual tide. The tidal level input in the PRD-LTMM-10 model consists of a representative tide.

2.1.2 *Simplification of the Physical System*

A number of basic premises for long-term simulation simplification were proposed by de Vriend *et al*. (1993) and Latteux (1995).

(1) The call times of the most time-consuming modules (current, wave and sediment transport

sometimes) are reduced by extending the topographic time step.

(2) A simplification method for flow fields or wave field upgrades (continuous modification) is introduced when modeling small changes in bed topography.

(3) The semi-empirical mean algorithm is used to model events/processes at small temporal and spatial scales.

(4) Overall parameterization and structure of the model.

A range of reduction methods are applied to processes occurring over different time scales (hydrodynamic or topographic variation processes). The long-term topographic simulation based on the tidal process can be ignored occasionally. The extension of the topographic time step is an effective way to avoid topographic upgrade after each tidal calculation. Reduction technologies include the direct delay method, the time-center delay method, and the tidal extension delay method (O'brien, 1969). The PRD-LTMM-10 model incorporates the tidal extension delay method.

2.1.3 *Output Simplification*

Extraction of information for the topographic analysis of trends in long-term variation requires the elimination, or reduction of noise (including attenuation of number errors accumulated over long term). Long-term topographic simulation is the achievement of a high degree of stochasticity in a highly nonlinear system. Thus, such simulations typically introduce a significant amount of noise, either masking or completely replacing the information of interest. Given this, accurate filter simplification is essential to the output of the model (Yang *et al*., 1995).

2.2 Model Modules

Not all physical processes and applicable aspects can be stimulated by use of long-term topographic simulation and calculation. Each computing module is based on certain physical approximation and parameterization rules. The morphodynamic model PRD-LTMM-10 includes a two-dimensional hydrodynamic tidal current module, a two-dimensional suspended sediment transport module, a bed deformation module, a riprap and siltation promotion module, and a waterway dredging module under the influence of simulated human behaviors. The relationship between these modules is illustrated in Fig. 1.

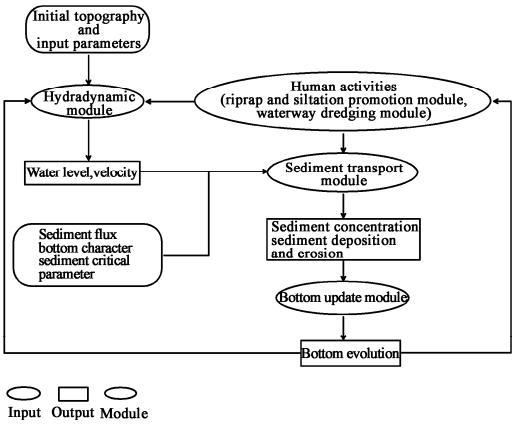

Fig. 1. Coupling diagram of all functional modules in the long-term model PRT-LTMM-10.

2.2.1 *2D Hydrodynamic Tidal Current Module*

Only the combined effect of tides and rivers is considered in this morphological model. The role of nearshore estuarine waves on estuarine evolution in the Pearl River Delta is considered to be secondary compared with that of tides and rivers (Luo *et al*., 2002). Thus, the wave effect is not included in the current model. Similarly, the baroclinic effect is also considered secondary relative to that of barotropy in general. The module also takes into account the need to reduce computational requirements. The flow movement control equations are represented by a continuity equation and a two-dimensional transport equation as follows:

$$\frac{\partial \eta}{\partial t}+\frac{\partial (Hu)}{\partial x}+\frac{\partial (Hv)}{\partial y}=0\,; \tag{1}$$

$$\frac{\partial u}{\partial t}+u\frac{\partial u}{\partial x}+v\frac{\partial u}{\partial y}=-g\frac{\partial \eta}{\partial x}+fv-gu\frac{\sqrt{u^2+v^2}}{c^2H}\,; \tag{2}$$

$$\frac{\partial v}{\partial t}+u\frac{\partial v}{\partial x}+v\frac{\partial v}{\partial y}=-g\frac{\partial \eta}{\partial x}-fu-gv\frac{\sqrt{u^2+v^2}}{c^2H}\,, \tag{3}$$

where, η is the tidal level; $H=h+\eta$ is the total water depth; h is the water depth under the base surface; u and v are the velocity components in x- and y- direction, respectively; g is the acceleration of gravity; f is the Coriolis coefficient ($2\Omega\sin\varphi$); c is the Chezy coefficient ($c=\frac{1}{n}(h+\eta)^{1/6}$); n is the Manning coefficient.

2.2.2 *Sediment Transport Module*

The plane 2D suspended sediment continuity equation is represented as:

$$\frac{\partial (HS)}{\partial t}+\frac{\partial (HuS)}{\partial x}+v\frac{\partial (HvS)}{\partial y}+\alpha\omega(S-S_*)=\frac{\partial}{\partial x}\left(\varepsilon_x H\frac{\partial S}{\partial x}\right)+\frac{\partial}{\partial y}\left(\varepsilon_y H\frac{\partial S}{\partial y}\right), \tag{4}$$

where, S and S_* are suspended sediment concentration and sediment transport capacity, respectively; α and ω are the coefficient of saturation recovery (settlement probability) and settling velocity, respectively; ε_x and ε_y are suspended sediment diffusion coefficients in x- and y- direction, respectively. The remaining symbols share the same definitions as above (Eqs. (1)~(3)).

2.2.3 *Bed Deformation Module*

The bed topographic deformation module was established through selection of a more common river bed deformation equation and the sediment transport capacity equation of Wuhan Institute of Hydraulics:

$$\gamma\frac{\partial \zeta}{\partial t}=\alpha\omega(S-S_*)\,; \tag{5}$$

$$S_*=k\left(\frac{V^3}{g\omega h}\right)^{m_0}, \tag{6}$$

where, ζ is the river bed elevation; γ is the dry bulk density of bed surface sediment; V is the vertical average velocity; g is the acceleration of gravity; k and m_0 are empirical coefficients. The

remaining symbols are defined above.

The integral is carried out to Eq. (5) (time is the integer multiple of tidal cycle *T*):

$$\int_0^{nT} \gamma \frac{\partial \zeta}{\partial t} \mathrm{d}T = n\gamma\overline{\zeta}; \tag{7}$$

$$\int_0^{nT} \alpha\omega\left(S - S_*\right)\mathrm{d}T = \overline{\alpha}\overline{\omega}\left(\overline{S} - \overline{S}_*\right)nT\ . \tag{8}$$

Resulting in:

$$\gamma\overline{\zeta} = \overline{\alpha}\overline{\omega}\left(S - \overline{S}_*\right)T\ . \tag{9}$$

The average scouring and silting thickness of suspended sediment in a tidal cycle may then be calculated as:

$$\overline{\zeta} = \frac{\overline{\alpha}\overline{\omega}}{\gamma}\left(\overline{S} - \overline{S}_*\right), \tag{10}$$

where, α is the settlement probability, and ω is the settling velocity of suspended sediment.

According to the above equation, the annual sedimentary thickness in a full tidal cycle (24 hours and 50 minutes) is shown as:

$$\zeta_{\text{year}} = 365\frac{24\text{h}00\,\text{min}}{24\text{h}50\,\text{min}}\overline{\zeta} \approx 352\frac{\overline{\alpha\omega}}{\gamma}(\overline{S} - \overline{S}_*)\ . \tag{11}$$

The variation in water depth caused by sediment compaction and neotectonic movement should also be considered. Thus, the water depth in the study area should be updated every six months to yield a two-dimensional flow field for the next sediment transport calculation. Because of a lack of data documenting sedimentary compaction and tectonic uplifting in the Modaomen Estuary, we did not conduct a calibration of sediment compaction and neotectonic induced changes in water depth in this study.

2.2.4 *Riprap and Siltation Promotion Module*

The purpose of riprap is to weaken water potential, confine flows to stabilize the river channel, and trap sands for silting and acceleration of beach siltation. Riprap embankments do not completely cut off water and sediment movement. Thus, borrowing from simulation models of gas-permeable walls for aircraft design and aerodynamics, we used permeable grid lines to simulate the actual role of riprap embankments. The width of the riprap embankment is negligible relative to its length, so that the width of the riprap is ignored in the simulation. Hence, the riprap embankment is replaced by computational grid lines. The computational grid lines present a partial obstruction to water and sediment, but do not completely hinder permeable grid lines (shown in Fig. 2). The permeability capacity of the permeable grid lines is regulated by the permeability rate σ ($0 \le \sigma \le 1$). When σ=0, the grid lines represent an impermeable embankment. When σ=1, the grid lines represent general computing grids. Meanwhile, the magnitude of the permeability rate is related to the height of the water level at the riprap embankment. If the water level is lower than the height of the riprap embankment, the permeability rate σ will be the constant *C* (*C* is determined by multiple debugs). If the water level exceeds the height of the riprap embankment, the permeability rate will change with

water levels based on C.

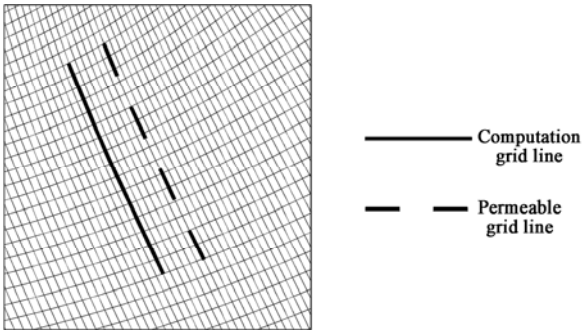

Fig. 2. Schematic diagram of permeable and computational grid lines.

2.3 Model Debug and Verification

Careful debugging and verification are required prior to application of the long-term model. Model debugging is conducted to adjust the parameters based on the statistical dispersion between model output and observational data under the given boundary conditions. This process is based strictly on physical laws. The millennial-scale long-term morphodynamic model requires a great deal of information for its calibration. Hence, verification occurs primarily by the analysis of geologic, sedimentary, and archaeological evidence (Wei *et al*., 2008). However, verification of the 10~100 year scale model can be achieved by comparison with historical topographic maps, nautical charts, and historical hydrological records.

3. Application of PRD-LTMM-10 Model

3.1 Overview of the Modaomen Estuary

The Modaomen Channel is the primary channel connecting the Pearl River to the sea (Fig. 3). It is the main channel of the Xijiang River and the multi-year average water and sediment yield for the channel account for 24.9% and 29%, respectively, of the total for the Pearl River.

Modaomen tides are irregular semidiurnal and the tidal range is about 1 m. Modaomen is characteristic of large runoff and small tide, which the average quantity of runoff is 5.77 times larger than tide. Generally, the tidal range in the dry season is larger than that in the flood season (Yang *et al*., 1995). The flow and sediment transport patterns differ significantly between the flood and dry seasons. A series of hills and islands are distributed in the neritic region and the surrounding of Modaomen.

3.2 Model Representative Input and Result Verification

3.2.1 *Model Input and Parameter Settings*

The model consists of an orthogonal curvilinear grid with 77 columns, 158 rows, and minimum mesh size of about 200 m. There are six open boundaries: Zhuyin and Huangjin represent two river boundaries, the open sea boundaries in the west, south, east, and at the exit to the Hongwan Channel. The measured open boundary data only cover the time of high and low tides and water level, where thrice spline interpolation is used for integral interpolation to satisfy the time interval required for

model calculation. No measured data exist in the open sea so the relevant data are obtained by extrapolation from the measured data at Sanzao Station based on micro-amplitude wave theory. The model uses moving boundary procedure techniques, where the water depth is H_0 = 0.1 m, determined by moving boundary wetting/drying.

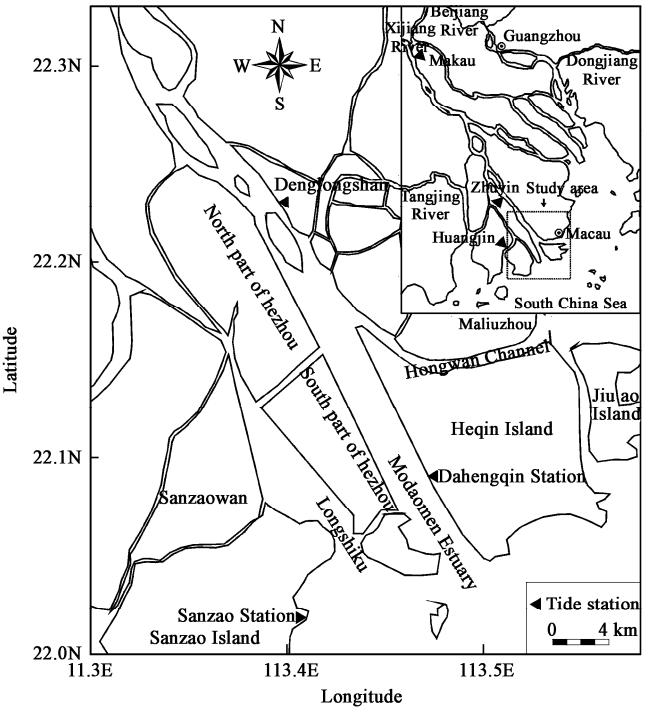

Fig. 3. The Modaomen Estuary.

The seasonal differences in river flow and sediment transport in the Modaomen Estuary are accounted for in the model representative input conditions. Given the lack of long-term data for these indices, representative sediment concentrations for the flood and dry seasons were obtained by use of multi-year average suspended sediment concentration, multi-year average flows, and the flow of the representative tide in flood and dry seasons. These data were supplemented with measured data and remote sensing images for comparison and modification. Following analysis and debugging, we used the tidal level curve from 9:00 on August 7 to 8:00 on August 22, 1981 to represent tidal input for the flood season in the model. Similarly, the tidal curve from 3:00 on March 1 to 2:00 on March 16, 1982 was used to represent tidal input for the dry season. The representative flow boundary for the flood season was 12163 m^3/s that of the dry season was 7768 m^3/s. The suspended sediment concentrations were 0.362 kg/m^3 and 0.060 kg/m^3 for the dry and flood seasons, respectively.

The model simulation began in 1977 and ended in 1988. The topography in 1977 represented the initial topographic boundary. The location of the riprap embankment was based on the 1:75000 “Chart of Xiaoputai Island to Xiaojin Island” measured in 1977 (Fig. 4).

The influences of extreme conditions (storms, typhoons, and other catastrophic weathers) are not considered in this model. The occurrence intensity and frequency of extreme events are difficult to

model over the long term. Although extreme conditions have very profound influences on the topography, the majority of catastrophic events occurring in the short term will tend to smooth under the equilibrium effect over a long time scale.

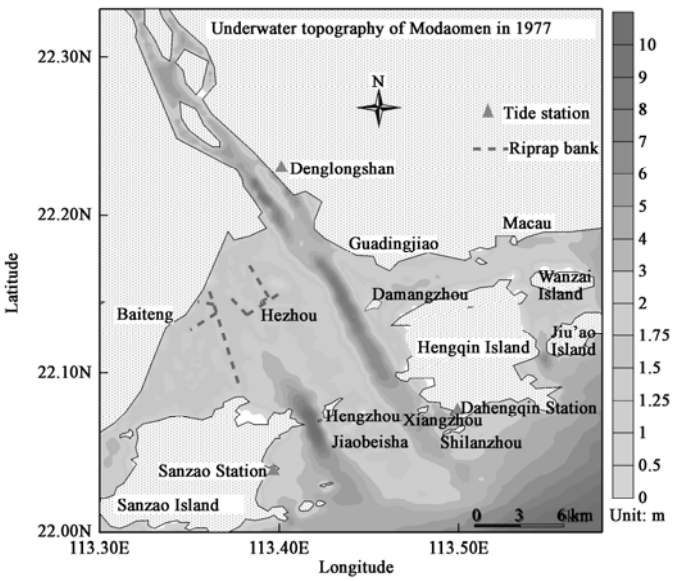

Fig. 4. Topography of the Modaomen Estuary in 1977 showing the location of the riprap embankment.

3.2.2 *Verification and Error Analysis of Calculated Results*

Verification of the model output occurs for measures of water level, velocity, total sediment transport, sedimentation amount, and sedimentation rate.

The verification of water level, velocity, and flow are directly related to the correct reflection of hydrodynamic characteristics in the study area by representative input conditions selected in the model. There is a long series of observational data for water levels and flow within the study area, allowing the verification of water levels and flow. However, the observational data for velocity and flow direction do not conform to the conventional requirements, resulting in problems verifying velocity and flow direction. In the case of insufficient information, the stimulation results of velocity and flow direction tend to be more reasonable than those for water level and velocity.

Multi-year hydrological data suggest that the diversion ratio for Zhuyin and Denglongshan Station in the Modaomen area (i.e., the percentage of net releasing water for these two stations relative to that of Makou Station) is about 1/3 (Luo *et al*., 2002). This value is primarily influenced and constrained by runoff, tide, and other factors. The model estimates for average flows at the Zhuyin Section between 1977 and 1988 are shown in Table 1. The average flow is 4110 m^3/s and 1732 m^3/s in the flood and dry seasons, respectively. The diversion ratio relative to Makau was 36.1% and 46.0%, respectively, which is lower than that in the analysis by Luo *et al*. (2002). Our results suggest that upland water in the model can represent the average runoff level for the Modaomen Estuary both in the flood and the dry seasons. Furthermore, the model input conditions were characterized by a strong representation.

Fig. 5 shows the comparison between the calculated and measured values for three hydrological stations (Denglongshan, Sanzao, and Dahengqin). The absolute average errors in water level are shown in Table 2 and are all smaller than 10 cm both in the flood and the dry seasons. In general, the error was smaller during the dry season than that in the flood season. Thus, the error was not only influenced by the selection of representative velocities and tides, but also by the lack of consideration for wind waves.

Table 1 Model estimates of the average flow in the Zhuyin Section between 1977 and 1988

	The average flow of Zhuyin Section (m^3/s)	The average flow of Makou (m^3/s)	Division ratio (Q_{Zhuyin}/Q_{Makau})
Flood season	4110	11400	36.1%
Dry season	1732	3770	46.0%

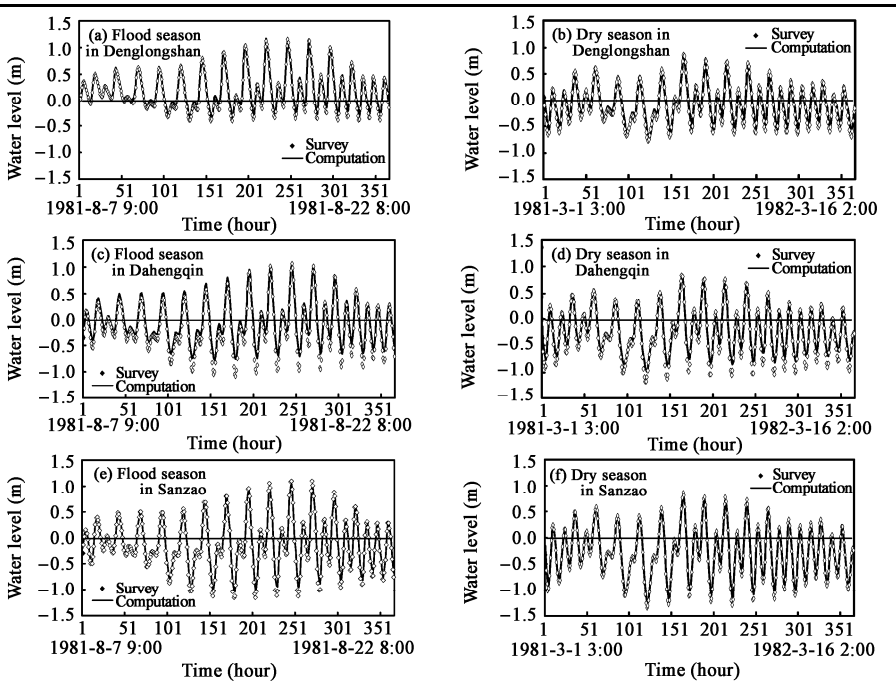

Fig. 5. Comparison between calculated and measured water level values in the flood and dry seasons; (a, b) Denglongshan Station, (c, d) Dahengqin Station, (e, f) Sanzao Station.

Table 2 Absolute average errors of water level at verified stations from 1977 to 1988 (cm)

Station	Denglongshan	Sanzao	Dahengqin
Flood season	5.3	5.4	9.5
Dry season	4.6	4.8	8.9

The representative input and output for suspended sediment in the model shall be consistent with the variations of suspended sediment in the study area.

Q_s is the suspended sediment flux input or output through boundaries with a time step of t_0–t_1, and S_i and $\vec{V}_i$ represent the vertical average suspended sediment concentration and velocity at the grid

points, respectively. Q_s shall be consistent with the total variation among the grid points (n is the total number) in the corresponding time interval.

The multi-year average sediment transport in the Modaomen Estuary was 23.41 million tons, accounting for 33% of the total sediment transport toward the sea (Zhao, 1990). The model estimates of annual average total sediment transport at Denglongshan Station in Modaomen from 1978 to 1988 were 23.46 million tons in flood season and 1.64 million tons in dry season (Table 3). The annual total was 25.1 million tons, accounting for 35.4% of the real total sediment transport into the sea.

Table 3 Model estimate of the total annual average sediment transport (1978~1988)

	Flood season	Dry season	Yearly total
The total annual average sediment transport of Denglongshan (10^4 t)	2346	164	2510
Sediment transport ratio of year (%)	93.5	6.5	100
The ratio of eight "gates" (%)		35.4	

3.2.3 *Verification of Sedimentation Amount and Rate*

The verification of this section was primarily conducted by comparison between the modeled results and historical charts. In the 1970s, riprap was installed in the North Hezhou and Sanzao Bay. The location of these riprap embankments was marked on a 1:75000 "Chart from Xiaoputai Island to Xiaojin Island" measured in 1977 (published by Navigation Guarantee Department of Chinese Navy Headquarters, People's Liberation Army, No. 15449) and in a 1:10000 "Planar Graph of the Hungwan-Modaomen Channel" surveyed from May to June, 1983. The specific locations are shown in Fig. 4. To facilitate the comparison of simulated results in the North Hezhou and Sanzao Bay before and after siltation, as well as the evolutionary analysis of siltation before and after the completion of governance and development projects in Modaomen, the study area was divided into four areas: the Sanzao Bay, North Hezhou, South Hezhou, and the Hongwan Channel (Fig. 6).

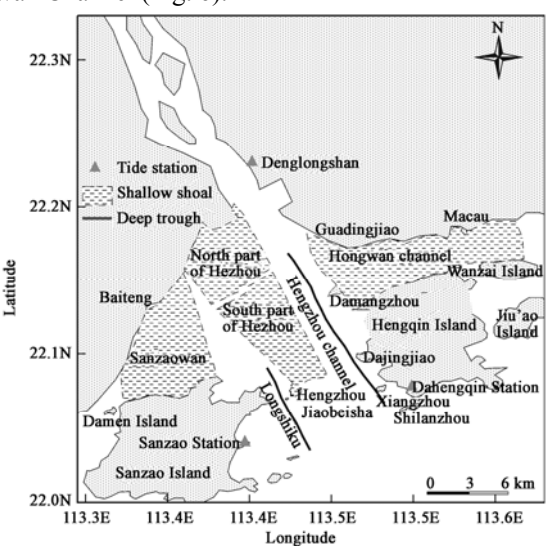

Fig. 6. Zoning of the study area.

The sedimentation rates for all riprap areas can be obtained by comparison between charts drawn in 1977 and 1983. The actual values for the three reclamation areas were between 3 and 5 cm/a with the sedimentary thickness of 0.18~0.29 m. A comparison between the simulated results and the charts suggests that both approaches yield similar overall trends in sedimentation and sedimentation amounts and rates with the error being smaller than 10% (Fig. 7, Table 4). The simulation error was the lowest for the Sanzao Bay (1.67%) and the highest for the South Hezhou and the Hongwan Channel. The roles of waves and the influences of extreme events were not considered in this model, which may have contributed to the large errors in these regions.

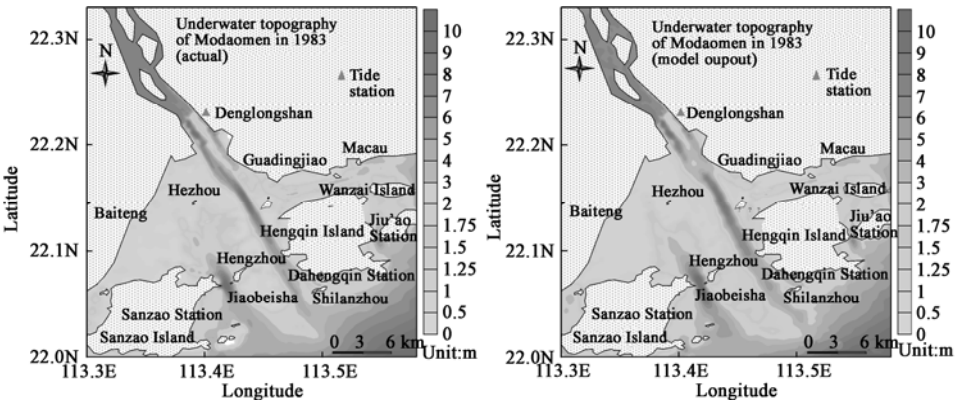

Fig. 7. Comparison between the topography of the Modaomen Estuary in 1983 calculated by the model and the actual topography.

Table 4 Comparison of deposition depth and deposition rate between model output and chart values (1977~1983)

Section of study area	Area (km^2)	Deposition depth (m)				Deposition rate (cm/a)				
		Model result			Result from chart	Model result			Result from chart	Relative error (%)
		Half-year of flood season	Half-year of dry season	Whole year		Half-year of flood season	Half-year of dry season	Whole year		
Sanzaowan	35.25	0.28	0.01	0.23	0.29	4.6	0.1	4.7	4.8	1.7
North of Hezhou	18.55	0.28	0.03	0.31	0.29	4.6	0.5	5.1	4.8	6.3
South of Hezhou	29.20	0.17	0.02	0.19	0.18	2.9	0.3	3.2	3.0	6.6
Hongwan channel	30.78	0.25	0.02	0.28	0.26	4.2	0.4	4.6	4.3	7.0

3.3 Morphodynamic Evolution of the Modaomen Estuary

There were significant differences in the trends in hydrodynamics and siltation evolutionary trend of the Modaomen Estuary in time and space (Fig. 8). Our results suggest that there is considerable seasonal variation in siltation. The highest levels of siltation occurred during the flood season accounting for about 95% of the annual total. Conversely, there is a large amount of scouring in the dry season such that siltation during this season accounts for only about 5% of the annual total. The majority of siltation was concentrated in the west of the estuary. The thickness of siltation increased from 17 cm adjacent to the Hengzhou Channel to 30 cm in the Sanzao Bay. Before 1977, runoff and sediment transport were diluted in the neritic region of Modaomen. The continuous siltation and

reclamation of the inner sea of Modaomen has reduced the capacity for water and sediment reception. This, in turn, has slowed down the siltation in the inner sea and the Hongwan Channel. Following the closure of the North Hezhou and Sanzao Bay, scouring has occurred in the main trough of the Hengzhou Channel leading to the acceleration of the main trough out-shift. In addition, the upper end of the Longshiku Deep Trough has narrowed due to severe siltation. The intensity of siltation increased in the areas adjacent to the inner sea islands of Modaomen, including the regions adjacent to Hezhou Island, Mangzhou, and Hezhou Island. However, the existence of these bedrock islands results in the disruption of siltation in the inner sea area, rather than simple unidirectional development from land toward the sea.

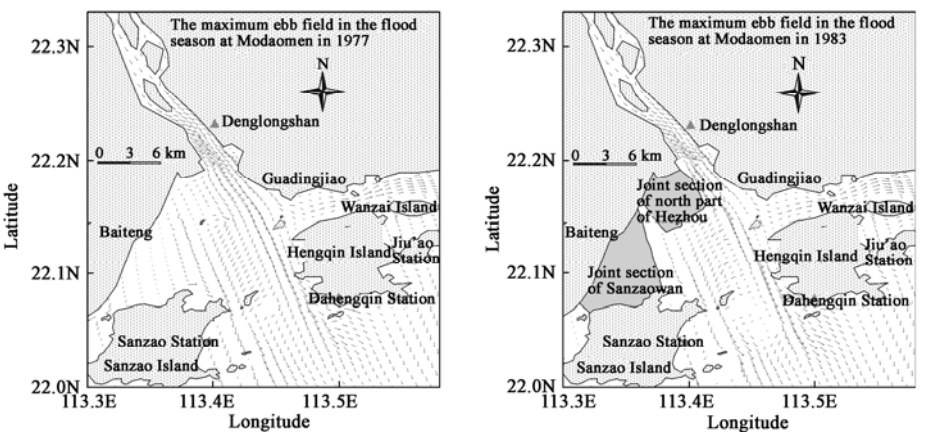

Fig. 8. Comparison of vector fields in 1977 and 1983.

4. Discussion

Ideally, estuaries would be preserved in their natural state. However, this is impractical because of the imbalance between demand and supply for coastal property. When flooding, waterlogging, salinization, storm surges, and other natural disasters occur in coastal areas, a range of engineering measures are introduced to reduce the recurrence of such events. However, these solutions are often associated with a new set of problems.

The natural factors influencing the evolution of the Modaomen Estuary over a 10~100 year period include estuarine morphology, the amount of water and sediment entering the estuary, tides and waves, sea-level rise, neotectonic movement, and ground subsidence. In addition, human activities are also an important factor controlling the geomorphologic evolution of the Modaomen Estuary. Human activities do not alter the laws of flow and sediment movement directly but do affect the boundaries, including the amount of incoming water and sediment, the diversion ratio, and the process of river networking and topographic boundaries of water flow movement. These boundaries are changed by human activities, leading to adjustment in the inherent movement law of water flow and sediment transport under the new boundary conditions.

We evaluated the influence of riprap and siltation in the Modaomen Estuary. Our results suggest

that riprap has a significant effect on sedimentation (Table 4, Table 5, and Fig. 9). The volume of incoming water and sediment is lower in the estuary in the dry season by an order of magnitude. Thus, riprap has a negligible effect on siltation during the dry season. The rate of natural siltation was only 2.81 cm/a in the South Hengzhou in the flood season, but increased to 4.6 cm/a after taking into account the role of the riprap embankment. The rate of sedimentation in the South Hezhou also increased by 8%. The total rate of sedimentation in the Sanzao Bay was relatively constant, but the area of aggregation moved eastward concentrating on the west side of riprap embankment. The South Hezhou is located in the lower reaches of the riprap embankment, so has less effect on siltation. The total sedimentation for the three reclamation areas following installation of riprap in the six months of the flood season increased from 2.924 million m^3 to 3.359 million m^3. The rate of siltation increased most rapidly in the North Hezhou. This is consistent with the morphodynamic characteristics of the Modaomen sea. The water is slowed down by the riprap embankments (Fig. 8), reducing the sediment carrying capacity when the runoff reaches the neritic region of the North Hezhou, resulting in rapid siltation of sediment entering the North Hezhou. Thus, the most rapid sedimentation occurs in the area surrounded by the 3 riprap embankments. In this area, more than 10 cm of sediment is deposited in the 6 months of the flood season. Interestingly, the thickness of siltation in the South Hezhou increased, even in the absence of riprap. However, due to the distance from the northern end of the riprap embankment, the rate of sedimentation is also lower. Thus, the morphodynamic processes associated with installation of riprap can be summarized as follows. (1) A reduction of velocity at the beach is conducive to siltation at the riprap embankment associated with sediment carried by flood tide. (2) Riprap prevents beach erosion by flood tides and floods, leading to difficulty in removing silt sediment. (3) The movement of bed load silt materials will be hindered on the east side of Hezhou, resulting in sedimentation occurring to bed load sediment in the lateral and front-ends of the riprap embankment. (4) Variations in beach sediment textures cause siltation of fine-grained sediment in the embankment.

Table 5 Validated results for deposition depth and deposition rate under natural processes (1977~1983)

Section of study area	Area (km^2)	Deposition depth (m)				Deposition rate (cm/a)				
		Model result			Result from chart	Model result			Result from chart	Relative error (%)
		Half year of flood season	Half year of dry season	Whole year		Half-year of flood season	Half-year of dry season	Whole year		
Sanzaowan	35.25	0.27	0.01	0.28	0.29	4.6	0.1	4.7	4.8	2.1
the North of Hezhou	18.55	0.17	0.03	0.20	0.29	2.81	0.5	3.3	4.8	31.0
the South of Hezhou	29.20	0.16	0.02	0.18	0.18	2.68	0.3	3.0	3.0	0.6
the Hongwan channel	30.78	0.26	0.03	0.29	0.26	4.5	0.4	4.8	4.3	11.6

We were able to simulate morphodynamic evolutionary processes in the Modaomen Estuary between 1977 and 1988 using the PRD-LTMM-10 model. The long-term influences of various human engineering activities and the roles of natural factors in estuarine evolution can be isolated by use of this long-scale

model. The morphodynamic evolution of the Modaomen Estuary has been heavily influenced by human activities (reclamation, siltation promotion, dredging, channel governance, etc.) in the last few decades. In this sense, the Modaomen Estuary has become an "artificial estuary".

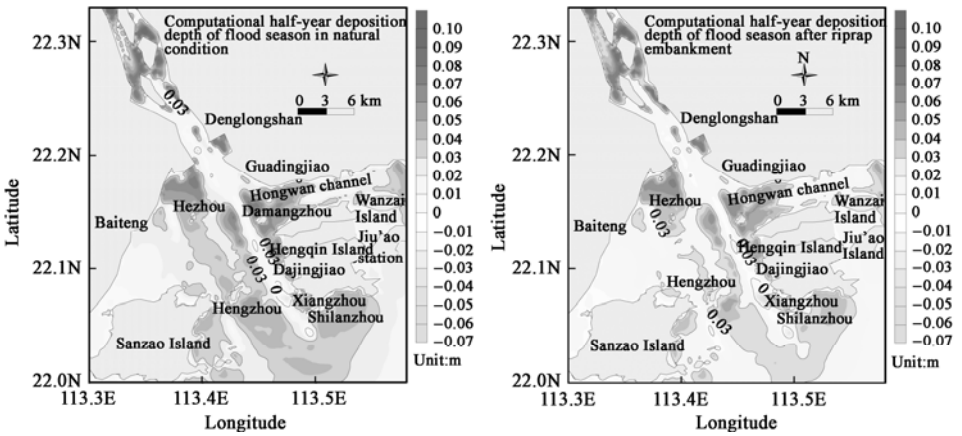

Fig. 9. Effect of riprap on siltation buildup during the six months of the flood season.

5. Conclusions

We simulated the morphodynamic evolution of the Modaomen Estuary between 1977 and 1988 using a long-term (10~100 year scale) estuarine "dynamics–sedimentation–morphology" model. The simulated results were consistent with observations from historical records. We achieved a reasonable separation between the long-term influences of human engineering activities and the roles of natural factors in the evolution of the estuary. Thus, the model is a powerful tool for the study of estuarine evolution and the assessment of the long-term effects of human activities.

Our results suggest that the governance projects had the largest effect on the natural development of the estuary. As a result of installing riprap and reclamation of submerged land, scouring occurred on the main Hengzhou Channel resulting in deep trough out-shift. Severe siltation caused a narrowing of the upper end of the Longshiku Deep Trough. Estuarine siltation in flood season accounted for about 95% of the annual total with the majority of siltation occurring in the west.

References

Stanica, A., Dan, S. and Ungureanu, V. G., 2007. Coastal changes at the Sulina mouth of the Danube River as a result of human activities, *Mar. Pollut. Bull.*, **55**(10-12): 555~563.

Jaffe, B. E., Smith, R. E. and Foxgrover, A. C., 2007. Anthropogenic influence on sedimentation and intertidal mudflat change in San Pablo Bay, California: 1856-1983, *Est. Coast. Shelf Sci.*, **73**(1-2): 175~187.

Bruun, P. and Gerritsen, F., 1960. *Stability of Coastal Inlets*, North Holland Pub. Co., Amsterdam, 1~123.

Dean, R. G., 1991. Equilibrium beach profiles: characteristics and applications, *J. Coast. Res.*, **7**(1): 53~84.

De Vriend, H. J., Zyserman, J. and Nicholson, J., 1993. Medium-term 2DH coastal area modeling, *Coast. Eng.*, **21**(1-3): 193~224.

Latteux, B., 1995. Techniques for long-term morphological simulation under tidal action, *Mar. Geol.*, **126**(1-4):

129~141.

Luo, X. L., Yang, Q. S. and Jia, L. W., 2002. *The Riverbed Evolution of the Pearl River Delta Network*, Sen Yat-Sen University Press, Guangzhou, 3~132. (in Chinese)

O'brien, M. P., 1969. Equilibrium flow areas of inlets on sandy coasts, *Proc. ASCE, J. Waterw. Harbours Coast. Eng.*, 15, 43~52.

Pritchard, D., Hogg, A. J. and Roberts, W., 2002. Morphological modelling of intertidal mudflats: the role of cross-shore tidal currents, *Cont. Shelf Res.*, **22**(11-13): 1887~1895.

Quiquerez, A., Allemmand, P. and Dromart, G., 2000. A 3-D two-lithology diffusive model for basin infilling, *Computers and Geosciences*, **26**(9-10): 1029~1042.

Ren, J. and Wu, C. Y., 2006. Representative conditions in the long-term morphodynamic model, *Advances in Water Science*, **17**(2): 278~282. (in Chinese)

Simon, J. B., Kenneth, P., van der Wal, D. and Adrian, N., 2006. Long-term morphological change and its causes in the Mersey Estuary, NW England, *Geomorphology*, **81**(1-2): 185~206.

Townend, I., 2005. An examination of empirical stability relationships for UK estuaries, *J. Coast. Res.*, **21**(5): 1042~1053.

van der Wal, D., Pye, K. and Neal, A., 2002. Long-term morphological change in the Ribble Estuary, northwest England, *Mar. Geol.*, **189**(3-4): 249~266.

Wei, X., Wu, C. Y. and Ren, J., 2008. A numerical simulation and mophodynamic analysis on the evolution of the drowned valley bay of Guangzhou since 6 ka, *Science in China Series D*: *Earth Sciences*, **38**(11): 1384~1395. (in Chinese)

Whitehouse, R. J. S., 2001. Predicting estuary morphology and process: an assessment of tools used to support estuary management, *Proceedings of the Seventh International Conference on Estuarine and Coastal Modelling*, St. Petersburg, Florida, USA, November 5-7, 344~363.

Wu, C. Y., Bao, Y. and Ren, J., 2006a. A numerical simulation and mophodynamic analysis on the evolution of the Zhujiang River Delta in China: 6000-2500 a BP, *Acta Oceanologica Sinica*, **4**, 64~80. (in Chinese)

Wu, C. Y., Ren, J., Bao, Y., Shi, H. Y., Lei, Y. P., He, Z. G. and Tang, Z. M., 2006b. A preliminary study on the morphodynamic evolution of the 'gate' of the Pearl River Delta, China, *Acta Geographica Sinica*, **61**(5): 537~548. (in Chinese)

Wu, C. Y., Ren, J., Bao, Y., Shi, H. Y. and Lei, Y. P., 2007a. A long-term morphological modeling study on the evolution of the Pearl River Delta, and estuarine bays since 6000 yr B.P., *The Geological Society of America*, Special Paper: 199~214.

Wu, C. Y., He, Z. G., Ren, J., Bao, Y., Mo, W. Y. and Wei, X., 2007b. A physical study on the evolution of the sub-delta plains in the mid Zhujiang River Delta: a case study of Da'ao sub-delta, *Quaternary Sciences*, **27**(5): 814~827. (in Chinese)

Yang, G. R., Li, C. C. and Luo, Z. R., 1995. *Coastal Morphodynamic Research and Its Application to Port Construction in South China,* Sen Yat-Sen University Press, Guangzhou, 243~277. (in Chinese)

Zhao, H. T., 1990. *The Evolution of the Pearl River Estuary*, China Ocean Press, Beijing, 1~357. (in Chinese)